MASTER'S DEGREE THESIS

Master of Science in Advanced Mathematics and Mathematical Engineering

Title: A C0 interior penalty method for 4th order PDE's

Author: Daniel Fojo Àlvarez

Advisors: Sonia Fernández Méndez and David Codony Gisbert

Department: Enginyeria Civil i Ambiental

Academic year: 2019

UNIVERSITAT POLITÈCNICA DE CATALUNYA
BARCELONATECH
Facultat de Matemàtiques i Estadística

Universitat Politècnica de Catalunya
Facultat de Matemàtiques i Estadística

Master in Advanced Mathematics and Mathematical Engineering

Master's thesis

A $\mathcal{C}^0$ interior penalty method for 4th order PDE's

Daniel Fojo Àlvarez

Supervised by Sonia Fernández and David Codony

June, 2019

Abstract

Fourth order Partial Differential Equations (PDE's) arise in many different physic's fields. As an example, the research group for Mathematical and Computational Modeling at UPC LaCàN is studying flexoelectricity, a very promising field which aims to replace some of the uses of piezoelectric materials, and whose equations involve 4th order derivatives. This work provides a method to solve these 4th order PDE's using the Finite Element Method (FEM) with $\mathcal{C}^0$ elements, which provides many advantages with respect to other methods that involve using $\mathcal{C}^1$ elements or decoupling the equation. The method is developed over the equations of the deformation of a Kirchoff plate, which is also a 4th order PDE. This method is then successfully validated with numerical experiments, both physical and artificial. An analysis of the convergence as well as the method's sensitivity to a newly added parameter is also provided. Due to the success of the method, LaCàN group will use this method to solve flexoelectricity's PDE's.

1. Introduction

Partial Differential Equations (PDE's) with 4th order derivatives arise in many physics fields. At LaCàN research group numerical tools for the resolution of flexoelectricity problems (electroactive materials) [CMFMA19] are being developed. The equations of flexoelectricity are 4th order PDE's, so it's weak form involves second derivatives. This means that the standard Finite Element Method (FEM) with $\mathcal{C}^0$ elements cannot be used. Nowadays, these equations are being solved with $\mathcal{C}^1$ approximations over structured meshes, known as b-splines. These approximations have some limitations, namely, they have to use embedded boundaries for non-rectangular domains, ill-conditioning problems...

The focus of this work is the development of a suitable formulation for the solution of 4th order PDE's using $\mathcal{C}^0$ standard FEM approximations, and imposing $\mathcal{C}^1$ continuity in weak form. As a proof of concept the formulation is developed and tested for a simpler, but similar, 4th order PDE: the Kirchoff plate problem, which is a 1-dimensional equation that models the deformation of a plate.

The developed formulation is based on the ideas of the Interior Penalty Method (IPM) [Arn82], which considers discontinuous approximations and imposes $\mathcal{C}^0$ continuity in weak form for second order PDEs. Here, the same ideas are applied for 4th order PDE's, but considering $\mathcal{C}^0$ approximations and imposing the continuity of the derivative in weak form. It is worth mentioning that the resulting weak form involves in this case second order derivatives, two different types of Dirichlet and Neumann boundary conditions and punctual forces on corners of the boundaries. The derivations of the weak form will also require the use of the surface divergence theorems.

The document is structured as follows. The basics of the standard FEM method are recalled next in subsection 1.1, in the context of second order PDE's. The formulation for 4th order PDE's (in this work for the Kirchoff plate problem) is developed in Section 2, including the problem statement and the derivation of the weak form, as well as an analysis of the behaviour of a parameter that arises in the formulation of the weak form. In Section 3 we provide the results of multiple numerical experiments that validate our formulation form Section 2, as well as an analysis of the method's convergence and sensitivity to the aforementioned parameter. Finally, the conclusions of this work are stated in Section 4, which include the knowledge I acquired for this work in 4.1.

1.1 Finite Element Method

To recall the basics of the Finite Element Method (FEM) let us consider the following 2nd order elliptic problem:

$$-\Delta u = f \text{ on } \Omega \tag{1a}$$

$$u = u_D \text{ on } \partial\Omega \tag{1b}$$

The weak form of the problem is: find $u \in \mathcal{H}^1_0(\Omega) + \psi$ such that

$$a(u, v) = \ell(v) \ \forall v \in \mathcal{H}^1(\Omega) \tag{2}$$

with

$$a(u, v) = \int_\Omega \nabla u \cdot \nabla v \, d\Omega \tag{3a}$$

$$\ell(v) = \int_\Omega v f \, d\Omega \tag{3b}$$

$\psi \in \mathcal{H}_0^1(\Omega)$ such that $\psi = u_D$ on $\partial\Omega$, and $\mathcal{H}_0^1(\Omega) = \{v \in \mathcal{H}^1(\Omega) : v = 0 \text{ on } \partial\Omega\}$
The FEM solution, u^h, is obtained considering an approximation space, V^h, of $\mathcal{C}^0$ piece-wise polynomial functions based on a partition of Ω in elements. That is, solving the following problem: find $u^h \in V_0^h + \psi^h$ such that

$$a(u^h, v) = \ell(v) \; \forall v \in V_0^h \tag{4}$$

where $V_0^h \subset \mathcal{H}_0(\Omega)$.
In the Finite Element Method, V_0^h is usually P_k or Q_k, that is, the space of piece-wise polynomials of degree k with each piece being a triangle or a quadrilateral respectively. Then, V_0^h is a vector space generated by a finite set of basis functions $\{N_1, ..., N_n\}$, and the approximation can be written as

$$u \approx u^h = \sum_{i=1}^{n} u_i N_i \tag{5}$$

Now, finding the coefficients $\{u_i\}$ is equivalent to solving a linear system of equations.

$$\boldsymbol{K}\boldsymbol{u} = \boldsymbol{b} \tag{6}$$

with

$$K_{ij} = a(N_i, N_j) \tag{7a}$$
$$b_i = \ell(N_i) - a(N_i, \psi^h) \tag{7b}$$

where $\boldsymbol{u}$ is the vector with the coefficients $\{u_i\}$.
Further explanation of classical FEM can be found in [QQ09].
Note that since the weak form involves only first order derivatives, standard $\mathcal{C}^0$ finite element approximations can be considered, since $V^h \subset H^1(\Omega)$. This is not the case for 4th order PDE's, for which the weak form involves second order derivatives and therefore $\mathcal{C}^0$ FEM approximations may not be smooth enough. There are 3 main strategies to overcome this problem: 1) decouple the PDE in 2 second order PDE's, 2) consider $\mathcal{C}^1$ approximations, which can be done via interpolant method, such as Argyris triangular element [ADMS77] or Bogner-Fox-Schmit quadrilateral elements [BFS67], or via non-interpolant methods, such as using a b-spline basis [CMFMA19] or a mesh free method [APM+14] or 3) develop a proper weak form suitable for $\mathcal{C}^0$ approximations. Decoupling the PDE in 2 second order PDE's has an important overcost in number of unknowns. On the other hand, $\mathcal{C}^1$ approximations are difficult to define for unstructured finite element meshes. A comparison between $\mathcal{C}^0$ and $\mathcal{C}^1$ elements can be found in [BS05]. This work focuses on the third option: developing a formulation for $\mathcal{C}^0$ approximations imposing $\mathcal{C}^1$ continuity between elements in weak form.

2. An IPM-$\mathcal{C}^0$ method for Kirchoff plates

For this section we will use Einstein notation, where if an index appears twice in a single term and is not otherwise defined, it implies summation of that term over all the values of the index.
We want to solve the following Kirchoff plate problem:

$$\frac{\partial^2 \sigma_{ij}(u)}{\partial x_i \partial x_j} = f \text{ on } \Omega \tag{8a}$$
$$u = g_1 \quad \text{on } \Gamma_D^1 \tag{8b}$$
$$\frac{\partial u}{\partial \boldsymbol{n}} = g_2 \quad \text{on } \Gamma_D^2 \tag{8c}$$
$$t(u) = t_n \quad \text{on } \Gamma_N^1 \tag{8d}$$
$$r(u) = r_n \quad \text{on } \Gamma_N^2 \tag{8e}$$
$$j_k(u) = j_k^{\text{ext}} \quad \text{on } V_k \in V_N \tag{8f}$$

where

$$\sigma_{ij}(u) = C_{ijkl} \frac{\partial^2 u}{\partial x_k \partial x_l} \tag{9a}$$
$$t(u) = \left(\nabla^\tau \cdot (\boldsymbol{n}) n_i \sigma_{ij}(u) + \frac{\partial \sigma_{ij}(u)}{\partial x_i} \right) n_j - \nabla^\tau \cdot (\boldsymbol{\sigma} \cdot \boldsymbol{n}) \tag{9b}$$
$$r(u) = \boldsymbol{n} \cdot \boldsymbol{\sigma} \cdot \boldsymbol{n} \tag{9c}$$
$$j_k(u) = \boldsymbol{\tau_k^L} \cdot \boldsymbol{\sigma} \cdot \boldsymbol{n_k^L} + \boldsymbol{\tau_k^R} \cdot \boldsymbol{\sigma} \cdot \boldsymbol{n_k^R} \tag{9d}$$

$\Gamma_D^1 \cup \Gamma_N^1 = \Gamma_D^2 \cup \Gamma_N^2 = \partial\Omega$, V_N are the vertices of the boundary in Γ_N^1, $\boldsymbol{n}$ is the exterior unitary normal vector and $\boldsymbol{\tau}$ is the tangent vector. At each vertex, superscripts L and R refer to the left and right edge that meet there. An illustration of this can be seen in Figure 1.

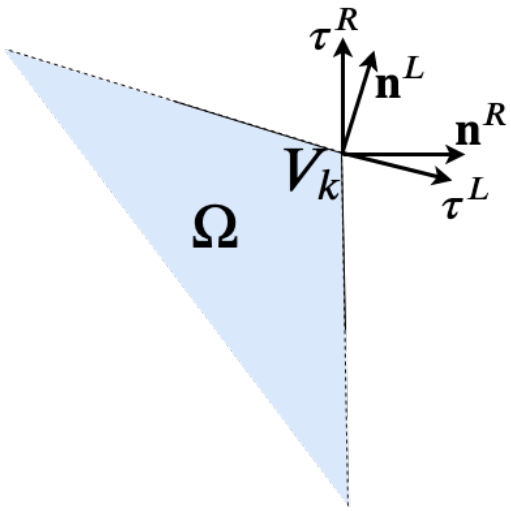

Figure 1: Left and right tangent and normal vectors at a corner of the domain.

$\nabla^\tau = \boldsymbol{\tau}\frac{\partial}{\partial \boldsymbol{\tau}} = \boldsymbol{\tau}(\boldsymbol{\tau}\cdot\nabla)$, g_1 and g_2 are prescribed variables for the displacement u and its normal derivative, t_N and r_N are given forces on the boundary, and f is an applied force.

2.1 Weak Form

Let's consider now a partition of Ω in subdomains Ω_e called elements, and

$$\widehat{\Omega} = \bigcup_e \Omega_e \tag{10a}$$

$$\widehat{\Gamma_D^1} = \bigcup_e \left(\overline{\Omega_e} \cap \Gamma_D^1\right) \tag{10b}$$

$$\widehat{\Gamma_N^1} = \bigcup_e \left(\overline{\Omega_e} \cap \Gamma_N^1\right) \tag{10c}$$

$$\widehat{\Gamma_D^2} = \bigcup_e \left(\overline{\Omega_e} \cap \Gamma_D^2\right) \tag{10d}$$

$$\widehat{\Gamma_N^2} = \bigcup_e \left(\overline{\Omega_e} \cap \Gamma_N^2\right) \tag{10e}$$

Problem (8) can now be stated in the broken domain as

$$\frac{\partial^2 \sigma_{ij}(u)}{\partial x_i \partial x_j} = f \qquad \text{on } \widehat{\Omega} \tag{11a}$$

$$u = g_1 \qquad \text{on } \widehat{\Gamma_D^1} \tag{11b}$$

$$\frac{\partial u}{\partial \boldsymbol{n}} = g_2 \qquad \text{on } \widehat{\Gamma_D^2} \tag{11c}$$

$$t(u) = t_n \qquad \text{on } \widehat{\Gamma_N^1} \tag{11d}$$

$$r(u) = r_n \qquad \text{on } \widehat{\Gamma_N^2} \tag{11e}$$

$$j_k(u) = j_k^{\text{ext}} \qquad \text{on } V_k \in V_N \tag{11f}$$

$$[\![u\boldsymbol{n}]\!] = \left[\!\left[\frac{\partial u}{\partial \boldsymbol{n}}\right]\!\right] = \{r(u)\} = 0 \text{ on } \Gamma \tag{11g}$$

$$[\![t(u)]\!] = \mathbf{0} \qquad \text{on } \Gamma \tag{11h}$$

$$\sum_{e_i \in E_k} j_k^{e_i}(u) = 0 \qquad \text{on } V_k \in V_\Gamma \tag{11i}$$

where Γ is the union of all interior sides Γ_f,

$$\Gamma = \left[\bigcup_e \partial\Omega_e\right] \setminus \partial\Omega = \bigcup_f \Gamma_f \tag{12}$$

E_k is the set of elements Ω_{e_i} that touch the vertex V_k, V_Γ is the set of all the vertices in Γ, and the jump and mean operators are defined on each face Γ_f as

$$[\![a]\!] = a^L + a^R \tag{13a}$$

$$\{a\} = \frac{1}{2}\left(a^L + a^R\right) \tag{13b}$$

with a^L and a^R being the values from the elements Ω^L and Ω^R sharing the sides. Note that the jump operator is always used including the normal vector. For instance,

$$[\![u\boldsymbol{n}]\!] = u^L\boldsymbol{n}^L + u^R\boldsymbol{n}^R = (u^L - u^R)\boldsymbol{n}^L \tag{14}$$

which is zero for a continuous function. Thus, equations (11g), (11h) and (11i) impose continuity of the displacement and its normal derivative, equilibrium of internal forces across sides between elements and equilibrium of forces on internal vertices.
Now, multiplying equation (11a) by an arbitrary function v and integrating over any element Ω_e we get

$$\int_{\Omega_e} vf\, d\Omega = \int_{\Omega_e} v\frac{\partial^2\sigma_{ij}(u)}{\partial x_i \partial x_j}\, d\Omega$$

Using twice the following formula (integration by parts)

$$\int_{\Omega_e} a\frac{\partial b}{\partial x_i}\, d\Omega = -\int_{\Omega_e} \frac{\partial a}{\partial x_i} b\, d\Omega + \int_{\partial\Omega_e} abn_i\, dS \tag{15}$$

we obtain

$$\begin{aligned}\int_{\Omega_e} vf\, d\Omega &= -\int_{\Omega_e} \frac{\partial v}{\partial x_i}\frac{\partial\sigma_{ij}(u)}{\partial x_j}\, d\Omega + \int_{\partial\Omega_e} v\frac{\partial\sigma_{ij}(u)}{\partial x_j} n_i\, dS \\ &= \int_{\Omega_e} \frac{\partial^2 v}{\partial x_i \partial x_j}\sigma_{ij}(u)\, d\Omega - \int_{\partial\Omega_e} \frac{\partial v}{\partial x_i}\sigma_{ij}(u) n_j\, dS + \int_{\partial\Omega_e} v\frac{\partial\sigma_{ij}(u)}{\partial x_j} n_i\, dS\end{aligned}$$

Now, using

$$\frac{\partial u}{\partial x_i} = n_i\frac{\partial u}{\partial \boldsymbol{n}} + \tau_i\frac{\partial u}{\partial \boldsymbol{\tau}} \tag{16}$$

the following version of the divergence theorem

$$\int_{\partial\Omega_e} \nabla^\tau(a)\cdot(\boldsymbol{A}\cdot\boldsymbol{n})\, dS = \int_{\partial\Omega_e} \nabla^\tau\cdot(a\boldsymbol{A}\cdot\boldsymbol{n})\, dS - \int_{\partial\Omega_e} a\nabla^\tau\cdot(\boldsymbol{A}\cdot\boldsymbol{n})\, dS \tag{17a}$$

and the surface divergence theorem

$$\int_{\partial\Omega_e} \nabla^\tau\cdot(a\boldsymbol{A}\cdot\boldsymbol{n})\, dS = \int_{\partial\Omega_e} \nabla^\tau\cdot(\boldsymbol{n})(a\boldsymbol{A}\cdot\boldsymbol{n})\boldsymbol{n}\, dS + \sum_{\Gamma_e} a\left([\boldsymbol{\tau}\boldsymbol{A}\boldsymbol{n}]_0^{end}\right) \tag{17b}$$

where $\boldsymbol{A}$ is a matrix, a is a scalar function and $\boldsymbol{\tau}$ is the tangent vector to the element side $\Gamma_f \subset \partial\Omega_e$, we have

$$\begin{aligned}\int_{\Omega_e} vf\, d\Omega = &+ \int_{\Omega_e} \frac{\partial^2 v}{\partial x_i \partial x_j}\sigma_{ij}(u)\, d\Omega \\ &+ \int_{\partial\Omega_e} v\left[\left(\nabla^\tau\cdot(\boldsymbol{n})n_i\sigma_{ij}(u) + \frac{\partial\sigma_{ij}(u)}{\partial x_i}\right)n_j - \nabla^\tau\cdot(\boldsymbol{\sigma}\cdot\boldsymbol{n})\right] dS \\ &- \int_{\partial\Omega_e} \frac{\partial v}{\partial \boldsymbol{n}}\left[n_i\sigma_{ij}(u)n_j\right] dS \\ &- \sum_{k=1}^{\#vertices} v\left(\boldsymbol{\tau}_{\boldsymbol{k}}^{\boldsymbol{L}}\sigma_k^e\boldsymbol{n}_{\boldsymbol{k}}^{\boldsymbol{L}} + \boldsymbol{\tau}_{\boldsymbol{k}}^{\boldsymbol{R}}\sigma_k^e\boldsymbol{n}_{\boldsymbol{k}}^{\boldsymbol{R}}\right)\end{aligned}$$

An illustration of the tangent and normal vectors for a face inside the mesh is provided in Figure 2, and an illustration of the tangent and normal vectors for a vertex of an element inside the mesh can be seen in Figure 3.

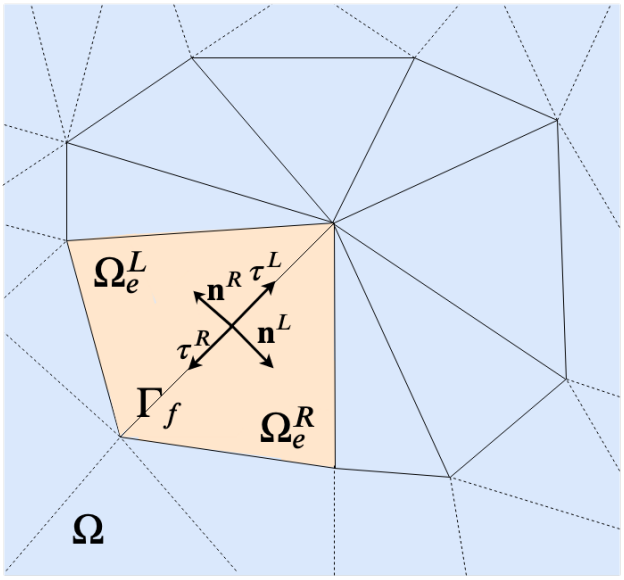

Figure 2: Left and right tangent and normal vectors for a face Γ_f inside the mesh.

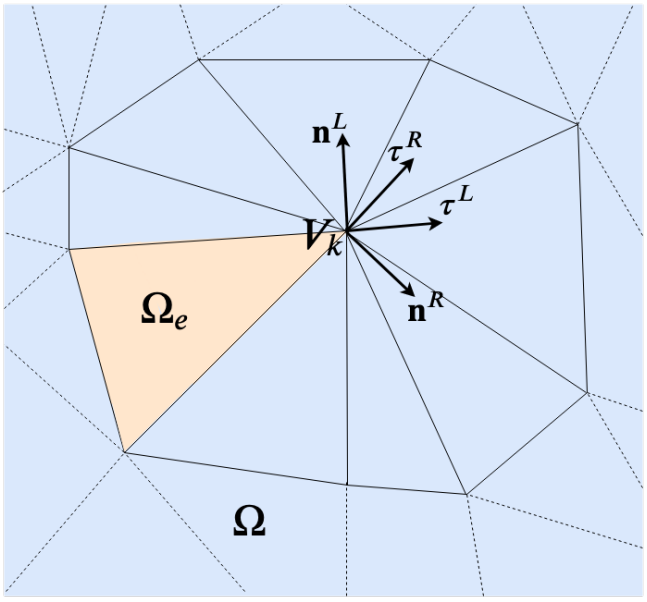

Figure 3: Left and right tangent and normal vectors for an interior vertex of an arbitrary element Ω_e inside the mesh.

Now, applying definitions (9b), (9c) and (9d), the equation becomes

$$\int_{\Omega_e} vf\, d\Omega = \int_{\Omega_e} \frac{\partial^2 v}{\partial x_i \partial x_j}\sigma_{ij}(u)\, d\Omega + \int_{\partial\Omega_e} vt^e(u)\, dS - \int_{\partial\Omega_e} \frac{\partial v}{\partial \boldsymbol{n}} r^e(u)\, dS - \sum_{k=1}^{\#vertices} v j_k^e(u) \tag{18}$$

where a superscript e means that it is the value on the element Ω_e. Now, to obtain our final equation for the whole domain, we add up every element,

$$\begin{aligned}\int_{\widehat{\Omega}} vf\, d\Omega = &\int_{\widehat{\Omega}} \frac{\partial^2 v}{\partial x_i \partial x_j}\sigma_{ij}(u)\, d\Omega + \int_{\partial\Omega} vt(u)\, dS - \int_{\partial\Omega} \frac{\partial v}{\partial \boldsymbol{n}} r(u)\, dS \\ &+ \sum_f \int_{\Gamma_f} v\left(t^L(u) + t^R(u)\right)\, dS \\ &- \sum_f \int_{\Gamma_f} \left[\frac{\partial v^L}{\partial \boldsymbol{n}^L} r^L(u) + \frac{\partial v^R}{\partial \boldsymbol{n}^R} r^R(u)\right] dS \\ &- \sum_{V_k \in V_{\text{int}}} v \sum_{e_i \in E_k} j_k^{e_i}(u) - \sum_{V_k \in V_{\text{ext}}} v \sum_{e_i \in E_k} j_k^{e_i}(u)\end{aligned}$$

where V_{int}, V_{ext} are the set of interior and exterior vertices respectively. Since we have $\left(t^L(u) + t^R(u)\right) = [\![t(u)]\!] = 0$ because of equation (11h), and using

$$\frac{\partial v^L}{\partial \boldsymbol{n}^L} r^L(u) + \frac{\partial v^R}{\partial \boldsymbol{n}^R} r^R(u) = \left[\!\left[\frac{\partial v}{\partial \boldsymbol{n}}\right]\!\right] \{r(u)\} + \{\nabla v\} \cdot [\![\boldsymbol{n} r(u)]\!] + \{r(v)\} \left[\!\left[\frac{\partial u}{\partial \boldsymbol{n}}\right]\!\right] = \left[\!\left[\frac{\partial v}{\partial \boldsymbol{n}}\right]\!\right] \{r(u)\} \tag{19}$$

where we used equation (11g), we end up with

$$\begin{aligned}\int_{\widehat{\Omega}} vf\, d\Omega = &\int_{\widehat{\Omega}} \frac{\partial^2 v}{\partial x_i \partial x_j}\sigma_{ij}(u)\, d\Omega + \int_{\partial\Omega} vt(u)\, dS - \int_{\partial\Omega} \frac{\partial v}{\partial \boldsymbol{n}} r(u)\, dS \\ &- \int_{\Gamma} \left[\!\left[\frac{\partial v}{\partial \boldsymbol{n}}\right]\!\right] \{r(u)\}\, dS \\ &- \sum_{V_k \in V_{\text{int}}} v \sum_{e_i \in E_k} j_k^{e_i}(u) - \sum_{V_k \in V_{\text{ext}}} v \sum_{e_i \in E_k} j_k^{e_i}(u)\end{aligned}$$

Imposing now continuity from equations (11g) and (11h), and using the fact that punctual forces are at equilibrium on interior corners from equation (11i), we get

$$\begin{aligned}\int_{\widehat{\Omega}} vf\, d\Omega = &\int_{\widehat{\Omega}} \frac{\partial^2 v}{\partial x_i \partial x_j}\sigma_{ij}(u)\, d\Omega + \int_{\partial\Omega} vt(u)\, dS - \int_{\partial\Omega} \frac{\partial v}{\partial \boldsymbol{n}} r(u)\, dS - \sum_{V_k \in V_{\text{ext}}} v \sum_{e_i \in E_k} j_k^{e_i}(u) \\ &- \int_{\Gamma} \left[\!\left[\frac{\partial v}{\partial \boldsymbol{n}}\right]\!\right] \{r(u)\}\, dS\end{aligned}$$

To ensure symmetry and positive definiteness of the final matrix that will define our system of equations, we can add terms that are analytically zero to the equation. The symmetric term of $\int_\Gamma \left[\!\left[\frac{\partial v}{\partial \boldsymbol{n}}\right]\!\right] \{r(u)\}\, dS$ is $\int_\Gamma \{r(v)\} \left[\!\left[\frac{\partial u}{\partial \boldsymbol{n}}\right]\!\right] dS$, which is zero because of equation (11g). For the positive definiteness, we will add the term $\int_\Gamma \left[\!\left[\frac{\partial v}{\partial \boldsymbol{n}}\right]\!\right] \left[\!\left[\frac{\partial u}{\partial \boldsymbol{n}}\right]\!\right] dS$ (which is also zero because of equation (11g)) times a sufficiently large constant β_1. Adding these terms, the obtained weak form is

$$\int_{\widehat{\Omega}} vf\, d\Omega = \int_{\widehat{\Omega}} \frac{\partial^2 v}{\partial x_i \partial x_j}\sigma_{ij}(u)\, d\Omega + \int_{\partial\Omega} vt(u)\, dS - \int_{\partial\Omega} \frac{\partial v}{\partial \boldsymbol{n}} r(u)\, dS - \sum_{V_k \in V_{\text{ext}}} v \sum_{e_i \in E_k} j_k^{e_i}(u)$$
$$- \int_\Gamma \left[\!\left[\frac{\partial v}{\partial \boldsymbol{n}}\right]\!\right] \{r(u)\}\, dS - \int_\Gamma \{r(v)\} \left[\!\left[\frac{\partial u}{\partial \boldsymbol{n}}\right]\!\right] dS + \beta_1 \int_\Gamma \left[\!\left[\frac{\partial v}{\partial \boldsymbol{n}}\right]\!\right] \left[\!\left[\frac{\partial u}{\partial \boldsymbol{n}}\right]\!\right] dS$$

This method of making the matrix symmetric and positive definite is inspired by Discontinuous Galerkin Interior Penalty Methods, which impose continuity in a similar manner, which can be seen in [Arn82]. An analysis of the value of the parameter β_1 is provided in Subsection 2.3.
Finally, we need to impose the boundary conditions. Equations (11d), (11e) and (11f) can be imposed directly by substituting its values in the corresponding terms. The boundary condition of equation (11b) can be strongly imposed in our system of equations by prescribing the values of the nodal unknowns at the boundary. Equation (11c) can be weakly imposed by adding two more terms paired with $\int_{\Gamma_D^2} \frac{\partial v}{\partial \boldsymbol{n}} r(u)\, dS$: $\int_{\Gamma_D^2} r(v) \left(\frac{\partial u}{\partial \boldsymbol{n}} - g_2\right) dS$ and $\beta_2 \int_{\Gamma_D^2} \frac{\partial v}{\partial \boldsymbol{n}} \left(\frac{\partial u}{\partial \boldsymbol{n}} - g_2\right) dS$, which we can add since $\left(\frac{\partial u}{\partial \boldsymbol{n}} - g_2\right)$ is analytically zero. This will also ensure symmetry and positive definiteness respectively. Note that this condition comes with another parameter β_2.

$$\begin{aligned}\int_{\widehat{\Omega}} vf\, d\Omega = &\int_{\widehat{\Omega}} \frac{\partial^2 v}{\partial x_i \partial x_j}\sigma_{ij}(u)\, d\Omega + \int_{\Gamma_N^1} vt_n\, dS - \int_{\Gamma_N^2} \frac{\partial v}{\partial \boldsymbol{n}} r_n\, dS - \sum_{V_k \in V_{\text{ext}}} v j_k^{\text{ext}} \\ &- \int_\Gamma \left[\!\left[\frac{\partial v}{\partial \boldsymbol{n}}\right]\!\right] \{r(u)\}\, dS - \int_\Gamma \{r(v)\} \left[\!\left[\frac{\partial u}{\partial \boldsymbol{n}}\right]\!\right] dS + \beta_1 \int_\Gamma \left[\!\left[\frac{\partial v}{\partial \boldsymbol{n}}\right]\!\right] \left[\!\left[\frac{\partial u}{\partial \boldsymbol{n}}\right]\!\right] dS \\ &- \int_{\Gamma_D^2} \frac{\partial v}{\partial \boldsymbol{n}} r(u)\, dS - \int_{\Gamma_D^2} r(v) \left(\frac{\partial u}{\partial \boldsymbol{n}} - g_2\right) dS + \beta_2 \int_{\Gamma_D^2} \frac{\partial v}{\partial \boldsymbol{n}} \left(\frac{\partial u}{\partial \boldsymbol{n}} - g_2\right) dS\end{aligned} \tag{20}$$

This way of weakly imposing boundary conditions is known as Nitsche's method [Nit71], and is frequently used in FEM.

2.2 Discretization

As in Section 1, the weak form (20) can be written as: find $u \in \mathcal{H}_0^1(\Omega) + \psi$ such that

$$a(u, v) = \ell(v)\ \forall v \in \mathcal{H}^1(\Omega) \tag{21}$$

with

$$\begin{aligned} a(u, v) = &\int_{\widehat{\Omega}} \frac{\partial^2 v}{\partial x_i \partial x_j}\sigma_{ij}(u)\, d\Omega \\ &- \int_\Gamma \left[\!\left[\frac{\partial v}{\partial \boldsymbol{n}}\right]\!\right] \{r(u)\}\, dS - \int_\Gamma \{r(v)\} \left[\!\left[\frac{\partial u}{\partial \boldsymbol{n}}\right]\!\right] dS + \beta_1 \int_\Gamma \left[\!\left[\frac{\partial v}{\partial \boldsymbol{n}}\right]\!\right] \left[\!\left[\frac{\partial u}{\partial \boldsymbol{n}}\right]\!\right] dS \\ &- \int_{\Gamma_D^2} \frac{\partial v}{\partial \boldsymbol{n}} r(u)\, dS - \int_{\Gamma_D^2} r(v) \frac{\partial u}{\partial \boldsymbol{n}}\, dS + \beta_2 \int_{\Gamma_D^2} \frac{\partial v}{\partial \boldsymbol{n}} \frac{\partial u}{\partial \boldsymbol{n}}\, dS \end{aligned} \tag{22a}$$

$$\begin{aligned} \ell(v) = &\int_{\widehat{\Omega}} vf\, d\Omega - \int_{\Gamma_N^1} vt_n\, dS + \int_{\Gamma_N^2} \frac{\partial v}{\partial \boldsymbol{n}} r_n\, dS + \sum_{V_k \in V_{\text{ext}}} v j_k^{\text{ext}} \\ &- \int_{\Gamma_D^2} r(v) g_2\, dS + \beta_2 \int_{\Gamma_D^2} \frac{\partial v}{\partial \boldsymbol{n}} g_2\, dS \end{aligned} \tag{22b}$$

$\psi \in \mathcal{H}_0^1(\Omega)$ such that $\psi = g_1$ on Γ_D^1, and $\mathcal{H}_0^1(\Omega) = \{v \in \mathcal{H}^1(\Omega) : v = 0 \text{ on } \partial\Omega\}$
As before, the FEM solution, u^h, is obtained considering an approximation space, V^h, of piece-wise polynomial functions. Then, the problem becomes: find $u^h \in V_0^h + \psi^h$ such that

$$a(u^h, v) = \ell(v) \; \forall v \in V_0^h \tag{23}$$

where $V_0^h \subset \mathcal{H}_0(\Omega)$.
As in Section 1, our approximation will be

$$u \approx u^h = \sum_{i=1}^{n} u_i N_i \tag{24}$$

To find the coefficients $\{u_i\}$ we will solve linear system of equations

$$\boldsymbol{K}\boldsymbol{u} = \boldsymbol{b} \tag{25}$$

with

$$K_{ij} = a(N_i, N_j) \tag{26a}$$
$$b_i = \ell(N_i) - a(N_i, \psi^h) \tag{26b}$$

where $\boldsymbol{u}$ is the vector with the coefficients $\{u_i\}$ and $\{N_i\}$ are the basis functions of V_0^h.

2.3 Analysis of IPM parameter

We provide now an analysis of the method's behaviour with respect to the newly added parameter β_1. A good choice for this parameter is essential, since we need β_1 to be big enough to ensure coercivity, but a value too large would yield an ill-conditioned matrix. For this analysis, we will set $\Gamma_N^2 = \partial\Omega$, which eliminates the dependence on β_2, and $r_n = 0$. Because of this, we will refer to β_1 as β for this subsection. The condition for positive definiteness is $a(v, v) > 0 \, \forall v \in V_0^h + \psi^h$.
Let $A = \int_{\widehat{\Omega}} \frac{\partial^2 v}{\partial x_i \partial x_j} \sigma_{ij}(u) \, d\Omega \geq 0$. Then, using the fact that $\Gamma_N^2 = \partial\Omega$ and $r_n = 0$ we have

$$a(v, v) = A - 2\int_\Gamma \left[\!\left[\frac{\partial v}{\partial \boldsymbol{n}}\right]\!\right] \{r(v)\} \, dS + \beta \int_\Gamma \left[\!\left[\frac{\partial v}{\partial \boldsymbol{n}}\right]\!\right]^2 dS \tag{27}$$

Now, using Cauchy-Schwartz inequality we get:

$$a(v, v) \geq A - 2\left\| \left[\!\left[\frac{\partial v}{\partial \boldsymbol{n}}\right]\!\right] \right\|_{L^2(\Gamma)} \|\{r(v)\}\|_{L^2(\Gamma)} + \beta \left\| \left[\!\left[\frac{\partial v}{\partial \boldsymbol{n}}\right]\!\right] \right\|_{L^2(\Gamma)}^2 \tag{28}$$

Now, assume

$$\|\{r(v)\}\|_{L^2(\Gamma)}^2 \leq C^2 A \tag{29}$$

Then

$$a(v, v) \geq A - 2C\sqrt{A} \left\| \left[\!\left[\frac{\partial v}{\partial \boldsymbol{n}}\right]\!\right] \right\|_{L^2(\Gamma)} + \beta \left\| \left[\!\left[\frac{\partial v}{\partial \boldsymbol{n}}\right]\!\right] \right\|_{L^2(\Gamma)}^2 \tag{30}$$

Using Young's inequality $\left(ab \leq \frac{a^2}{2\varepsilon} + \frac{\varepsilon}{2} b^2 \, \forall a, b, \varepsilon > 0\right)$ we have

$$a(v, v) \geq \left[1 - \frac{C}{\varepsilon}\right] A + [\beta - C\varepsilon] \left\| \left[\!\left[\frac{\partial v}{\partial \boldsymbol{n}}\right]\!\right] \right\|_{L^2(\Gamma)}^2 \tag{31}$$

So our condition for positive definiteness is $1 - \frac{C}{\varepsilon} > 0$ and $\beta - C\varepsilon > 0$. This can be rewritten as just

$$\beta > C^2 \tag{32}$$

where C satisfies equation (29). Using that in the vector space $V_0^h + \psi^h$ we have

$$A = \boldsymbol{V}^T \boldsymbol{M} \boldsymbol{V} \text{ with } M_{kl} = \int_{\widehat{\Omega}} \frac{\partial^2 N_k}{\partial x_i \partial x_j} \sigma_{ij}(u)(N_l)\, d\Omega \tag{33}$$

$$\|\{r(v)\}\|^2_{L^2(\Gamma)} = \boldsymbol{V}^T \boldsymbol{K} \boldsymbol{V} \text{ with } K_{kl} = \int_{\Gamma} \{r(N_k)\}\{r(N_l)\}\, dS \tag{34}$$

where $\{N_i\}$ are the basis functions and $\boldsymbol{V}$ is a vector containing all the coefficients of v for these basis functions.
Then, defining the following eigenvalue problem

$$\boldsymbol{K}\boldsymbol{V} = \lambda \boldsymbol{M}\boldsymbol{V} \tag{35}$$

it follows that $\boldsymbol{V}^T \boldsymbol{K} \boldsymbol{V} \leq \lambda_{\max} \boldsymbol{V}^T \boldsymbol{M} \boldsymbol{V}$, or equivalently,

$$\|\{r(v)\}\|^2_{L^2(\Gamma)} \leq \lambda_{\max} A = C^2 A \tag{36}$$

So, the value for β must satisfy

$$\beta > \lambda_{\max} \tag{37}$$

with $\lambda_{\max}$ being the largest eigenvalue of problem (35). This analysis allows us to know the physical units of the lower bound of β, which will be the same as the ones for $\lambda_{\max}$, which are the same as the units for $\boldsymbol{\sigma}$.

3. Numerical Experiments

3.1 Convergence and sensitivity to penalty parameter

We expect the L_2 error of our method to behave like:

$$||u - u^h||_{L_2(\Omega)} = Ch^{p+1} \tag{38}$$

where C is a positive constant, h is the size of an element in the mesh and p is the degree of the polynomial approximation. The derivation of the order of the error can be found in [BS05].
To check the convergence of our method, we will solve the following equation, which has an analytical polynomial solution:

$$\frac{\partial^2 \sigma_{ij}(u)}{\partial x_i \partial x_j} = 6y \text{ on } \Omega \tag{39a}$$

$$u = g_1 \qquad \text{on } \partial\Omega \tag{39b}$$

$$r(u) = r_n \qquad \text{on } \partial\Omega \tag{39c}$$

with

$$\boldsymbol{\sigma}(u) = \frac{t^3}{12}\left(2\mu\mathcal{H}(u) + \overline{\lambda}\mathbb{I}\Delta(u)\right) \tag{40}$$

where $\mathcal{H}(u)$ is the Hessian matrix, which contains the second derivatives with respect x and y, $\Delta(u)$ is the laplacian and $\mathbb{I}$ is the identity matrix. We will fix $t = \overline{\lambda} = \mu = 1$ and take $\Omega = [0,1]^2$ as our domain. For boundary conditions, we set $\Gamma_D^1 = \Gamma_N^2 = \partial\Omega$. Then, we have in each edge

$$g_1 = x^4 y \text{ on } \partial\Omega \tag{41}$$

and

$$r_n = \begin{cases} 0 & \text{when } y = 0 \\ 3y & \text{when } x = 1 \\ x^2 & \text{when } y = 1 \\ 0 & \text{when } x = 0 \end{cases} \tag{42}$$

The solution to this problem is $u = x^4 y$, which we will use to check the convergence of our method.
Note that with this boundary conditions, the problem only depends on the new parameter of this method β_1, which we will refer to as β. The equation we are solving depends on this parameter, which can affect convergence if not chosen properly. We have seen in Subsection 2.3 that the value must be sufficiently high for the final matrix to be definite positive, but a value too large for β can cause large condition number of the system matrix which might spoil optimal convergence of the method. Instead of computing the lower bound value for β analytically, we give an analysis of the sensitivity of our method to changes in β. From equation (37) we know that the lower bound of β will be proportional to $t^3\mu/h$ where h is the size of an element of the mesh.
In Figure 4 we can see that for degrees 1 and 2, the method gives a poor convergence. This is probably caused due to locking, since we are imposing continuity and for the solution and its first derivative, and the elements do not have enough degrees of freedom to approximate the solution.
For degrees $p > 2$ we see optimal convergence for penalty parameter within a certain range ($10t^3\mu/h$ - $100t^3\mu/h$). A lower parameter does not ensure coercivity, and higher values get suboptimal convergence because of ill-conditioning, though the error is still reasonably low.

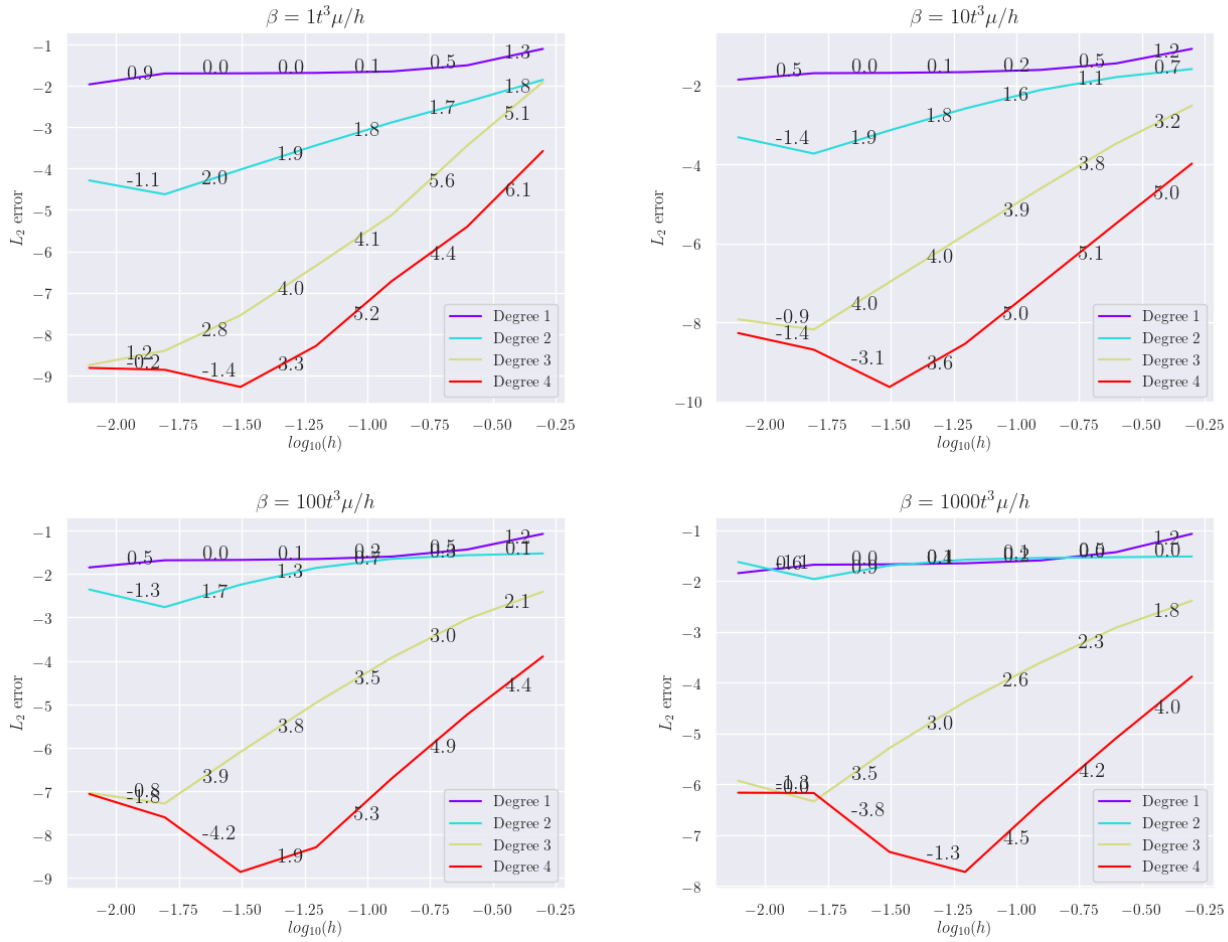

Figure 4: Convergence plots of our method for different values of β and different degrees p. The numbers indicated correspond to the slope of the line.

We also check the positive definiteness of the matrix of our system, by computing its smallest and largest eigenvalue. This can be seen in Figure 5. For a value of β greater than $10t^3\mu/h$, our system matrix is positive definite for any mesh size h and polynomial degree p. Finally, we check the condition number of the matrix for the values of β that give a positive definite matrix, which can be seen in Figure 6. We see that a value for β too large gives us an ill-conditioned matrix.

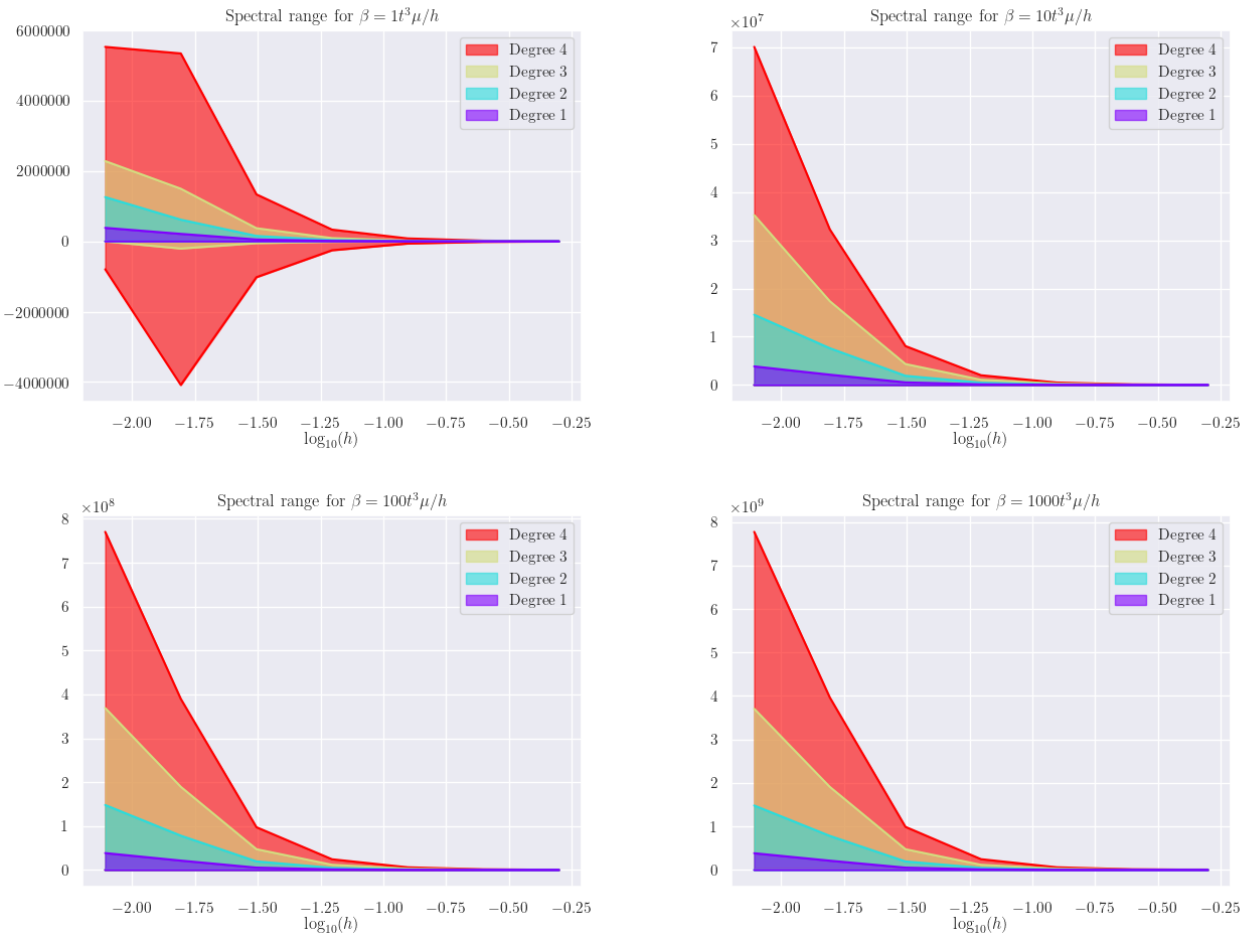

Figure 5: Plot of the spectral range for elements with degrees p 1 to 4 for different element sizes h. For values of β greater that $10t^3\mu/h$, the matrix is positive definite, since the minimum eigenvalue is always greater than 0.

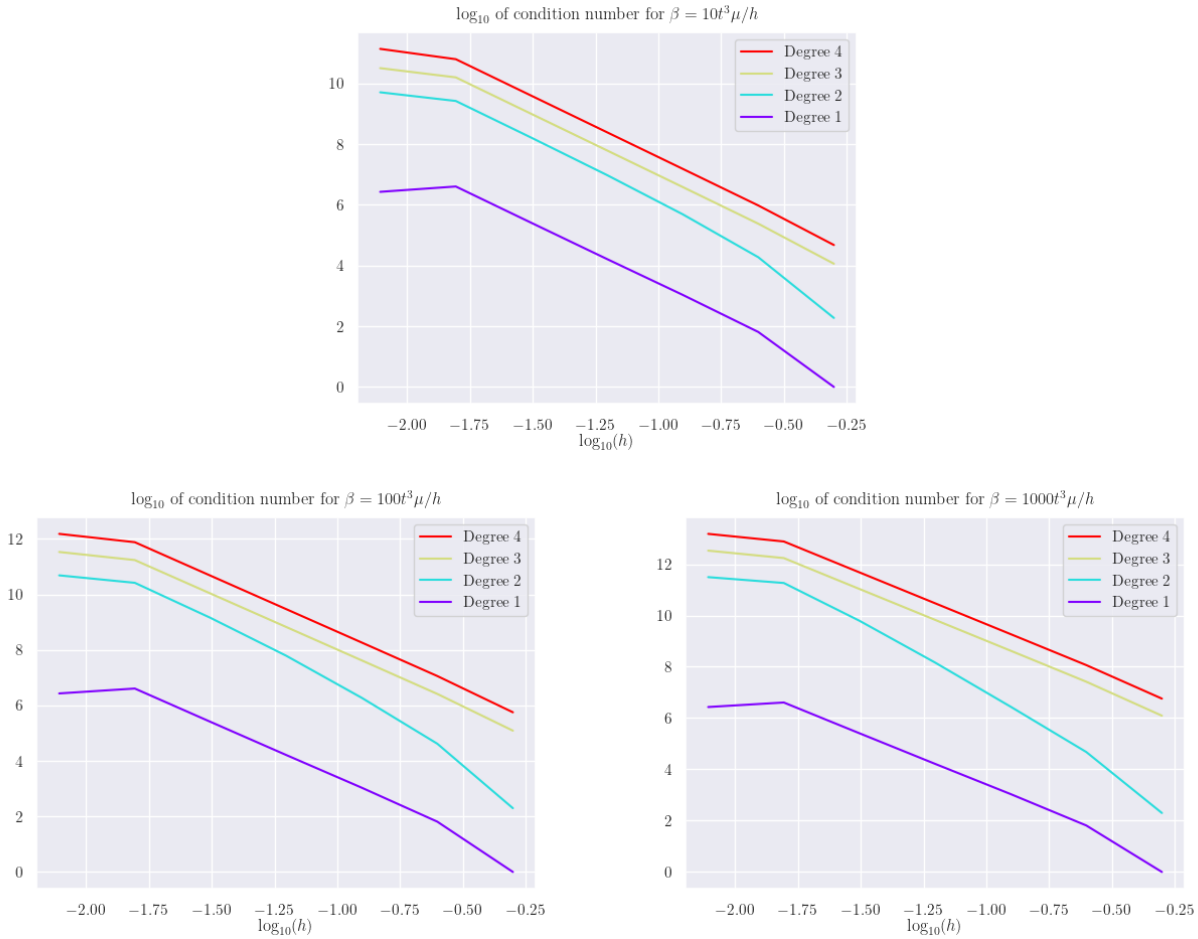

Figure 6: Plot of the condition number for degrees p 1 to 4 for different values of β with which the matrix is positive definite. We can see that a smaller valuer of β gives a lower condition number for all polynomial degree, which means that the method will be less prone to numerical errors.

3.2 Distributed load

We will use the method developed in Section 2 to solve the Kirchoff plate problem with a distributed load. Setting

$$\boldsymbol{\sigma}(u) = \frac{t^3}{12}\left(2\mu\mathcal{H}(u) + \overline{\lambda}\mathbb{I}\Delta(u)\right) \tag{43}$$

with

$$\mu = \frac{E}{2(1+\nu)} \tag{44a}$$

$$\overline{\lambda} = \frac{\nu E}{(1-\nu^2)} \tag{44b}$$

where t is the thickness of the plate, E is the Young's modulus, and ν is Poisson's ratio.

For the experiment, we will set the parameters to the ones of a 1mm thick steel plate taken from [MDH+01], that is,

$$t = 0.001\text{m} \tag{45a}$$
$$E = 200 \cdot 10^9\text{Pa} \tag{45b}$$
$$\nu = 0.28 \tag{45c}$$

and set the distributed load to $f = 100\text{Pa}$. The dimensions of the plate are of 1 by 1 meters. As for the penalty parameters, we will set $\beta_1 = \beta_2 = 10t^3\mu/h = (781.25\text{N m})/h$ where $h = 0.125\text{m}$ is the size of an element of the mesh. This problem is taken directly from [EGH+02].
We show both the solution for a simply supported plate ($\Gamma_N^2 = \partial\Omega$) in Figure 7 and the solution for a clamped plate ($\Gamma_D^2 = \partial\Omega$) in Figure 8. For these solutions, we used triangular elements of degree $p = 4$. In Figure 9 we can see the mesh that we used to find these solutions.

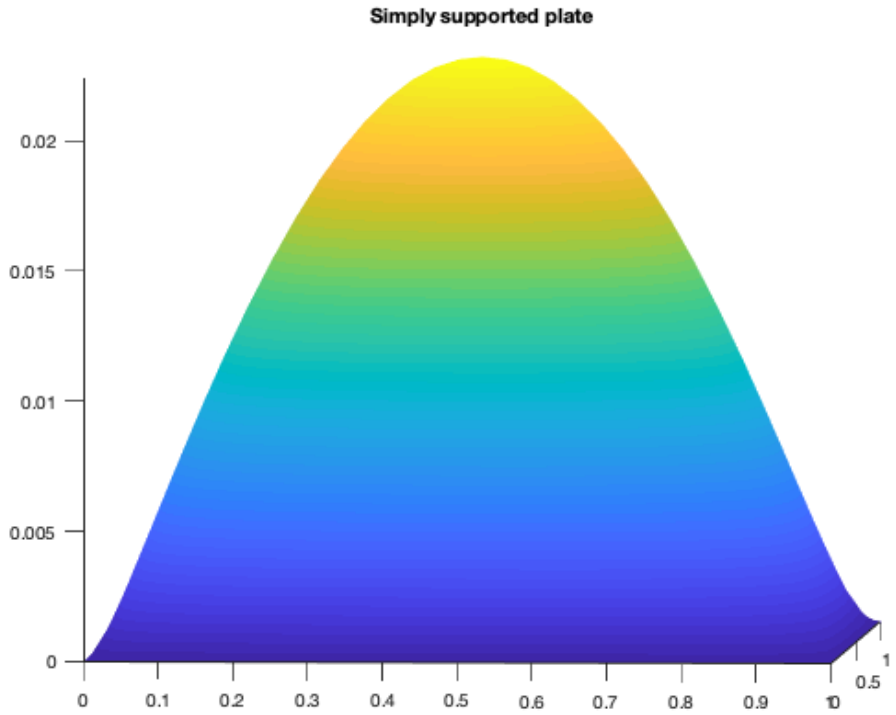

Figure 7: Solution of the problem with distributed load and second Neumann boundary condition ($\Gamma_N^2 = \partial\Omega$), which corresponds to a simply supported plate.

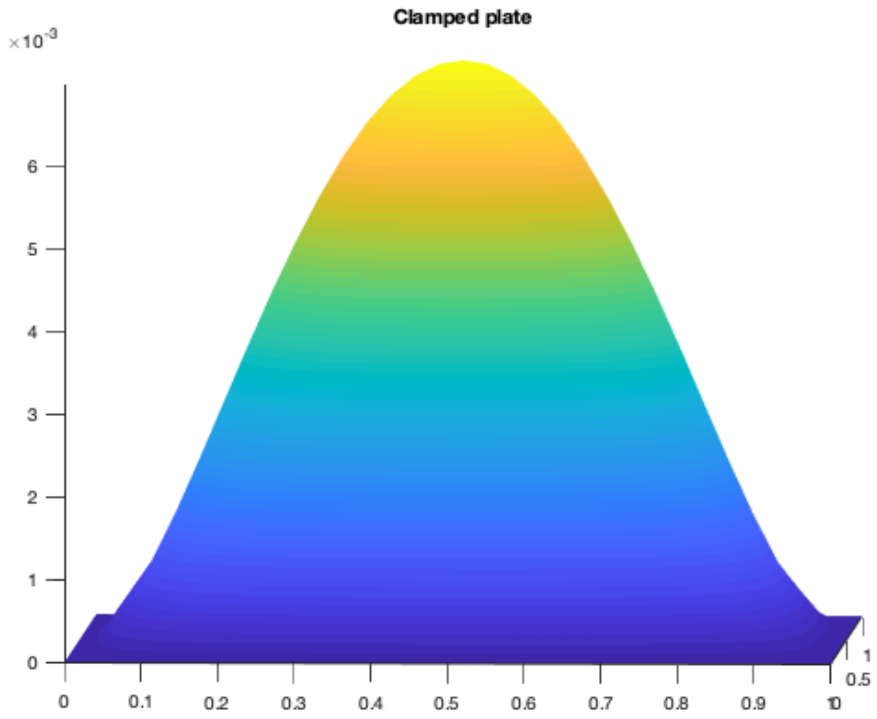

Figure 8: Solution of the problem with distributed load and second Dirichlet boundary condition ($\Gamma_D^2 = \partial\Omega$), which corresponds to clamped plate.

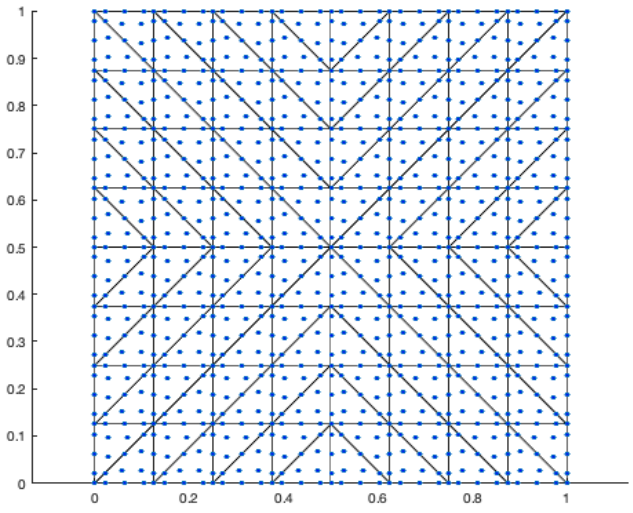

Figure 9: Mesh used to obtain the solutions of Figure 7 and 8. Each blue dot corresponds to a nodal value.

As we expected, we obtain a bigger maximum deformation for the simply supported plate (22.5mm) than with the clamped plate (7.0mm).

4. Conclusions

As a conclusion for this work, we developed a novel method to solve 4th PDE's numerically using $\mathcal{C}^0$ finite elements. We performed several numerical experiments to validate the method, which gave us successful results. This new way of solving 4th order PDE's provides many advantages over existing methods (which either used $\mathcal{C}^1$ elements, or decoupled the PDE in 2 second order PDE's) and will be used by the LaCàN group to solve problems with flexoelectricity.
This method depends on a new parameter β_1. We observed optimal convergence for a given range of this new parameter ($10t^3\mu/h$ to $100t^3\mu/h$ in our case). If the parameter is too low, we lose coercivity. If we fix the parameter to a value that is too large, we get suboptimal convergence due to ill-conditioning, but the method still provides acceptable errors. This means that our method is robust even without an optimal choice for β_1, as long as its value is large enough.
We observed that our method works best and achieves optimal performance when using elements of degree p at least 3. For degrees $p = 1$ and $p = 2$ the method seemed to lock, since the elements do not present enough degrees of freedom to impose continuity for the first derivative.
Finally, we also tested this method with a realistic physical problem, which gave us the expected results, further validating it.

4.1 Acquired knowledge

During my academic formation I only learnt the standard Finite Element Method described in 1.1. For this work, I had to get familiar with the interior penalty method for discontinuous elements, and then learn how to apply it to a 4th order PDE.
Then, an implementation of the new method had to be done. The standard implementation of FEM uses a reference element to compute the values of the matrix of the system, which does not include the value for the second order derivatives that we need for the formulation of the weak form, so these derivatives had to be implemented.
Furthermore, the equation of the weak form had to be implemented from scratch. This equation includes a term inside each element, two terms at each interior element face as seen from the left and right element, and one term at each exterior element face, so the computation of the matrix involved three different loops.
All the implementation was done using the MATLAB programming language, which I had to get familiar with, since I only used it sporadically during my education. The numerical experiments for the sensitivity to different values of β_1 and convergence were executed at a server in the LaCàN computer cluster, since it would have taken too long to execute them in a basic computer. Computing the smallest and largest eigenvalue of the matrix also involved using a special routine, since the matrices are very large and sparse.

References

[ADMS77] John Hadje Argyris, Padraic C Dunne, GA Malejannakis, and E Schelkle, *A simple triangular facet shell element with applications to linear and non-linear equilibrium and elastic stability problems*, Computer Methods in Applied Mechanics and Engineering **10** (1977), no. 3, 371–403.

[APM+14] Amir Abdollahi, Christian Peco, Daniel Millan, Marino Arroyo, and Irene Arias, *Computational evaluation of the flexoelectric effect in dielectric solids*, Journal of Applied Physics **116** (2014), no. 9, 093502.

[Arn82] Douglas N Arnold, *An interior penalty finite element method with discontinuous elements*, SIAM journal on numerical analysis **19** (1982), no. 4, 742–760.

[BFS67] FK Bogner, RL Fox, and LA Schmit, *A cylindrical shell discrete element.*, AIAA Journal **5** (1967), no. 4, 745–750.

[BS05] Susanne C Brenner and Li-Yeng Sung, *c_0 interior penalty methods for fourth order elliptic boundary value problems on polygonal domains*, Journal of Scientific Computing **22** (2005), no. 1-3, 83–118.

[CMFMA19] David Codony, Onofre Marco, Sonia Fernández-Méndez, and Irene Arias, *An immersed boundary hierarchical b-spline method for flexoelectricity*, CMAME **354** (2019), 750–782.

[EGH+02] G Engel, K Garikipati, TJR Hughes, MG Larson, Luca Mazzei, and Robert L Taylor, *Continuous/discontinuous finite element approximations of fourth-order elliptic problems in structural and continuum mechanics with applications to thin beams and plates, and strain gradient elasticity*, Computer Methods in Applied Mechanics and Engineering **191** (2002), no. 34, 3669–3750.

[MDH+01] Daniel B Miracle, Steven L Donaldson, Scott D Henry, Charles Moosbrugger, Gayle J Anton, Bonnie R Sanders, Nancy Hrivnak, Carol Terman, Jill Kinson, Kathryn Muldoon, et al., *Asm handbook*, vol. 21, ASM international Materials Park, OH, USA, 2001.

[Nit71] Joachim Nitsche, *Über ein variationsprinzip zur lösung von dirichlet-problemen bei verwendung von teilräumen, die keinen randbedingungen unterworfen sind*, Abhandlungen aus dem mathematischen Seminar der Universität Hamburg, vol. 36, Springer, 1971, pp. 9–15.

[QQ09] Alfio Quarteroni and Silvia Quarteroni, *Numerical models for differential problems*, vol. 2, Springer, 2009.